Use Of High Resolution CdZnTe M400 Modules In Safeguards

David Goodman[1], David Barron[1], Willy Kaye[1]

[1]H3D, Inc., Ann Arbor, Michigan

Abstract

Room-temperature, pixelated CdZnTe detectors offer the reliability of scintillators with spectral performance near that of high-purity germanium. Marrying these capabilities into a single, light-weight detector has the potential to greatly simplify the concept-of-operations for IAEA inspectors. The performance of an M400 CdZnTe detector is compared against current IAEA safeguards detectors and a modern, medium-resolution scintillator on plutonium and uranium standards. Results from an onboard uranium grading algorithm are benchmarked across a wide variety of enrichments and shielding. Potential use with the FRAMv6 package is discussed.

Introduction

Passive, non-destructive gamma-ray assay is commonly used to quantify plutonium and uranium isotopics in international safeguards. Low-resolution detectors, such as NaI scintillators, provide sufficient spectral information for constrained problems, such as enrichment meter measurements, where source geometries are well known [1]. In contrast, high-resolution detectors, such as high-purity germanium (HPGe), offer sufficient spectral information to characterize both uranium and plutonium samples in relatively unconstrained geometries using tools like FRAM and others [2][3][4]. However, high-resolution HPGe detectors come with the logistical burden of liquid nitrogen or maintenance on Stirling coolers. Recent advances in state-of-the-art CdZnTe detectors have produced near-HPGe quality single-pixel spectra (0.35 % FWHM at 662 keV) at room-temperature [5]. Previous analysis has shown that high-resolution CdZnTe spectra contain sufficient information for the unconstrained analysis of uranium, and potentially plutonium, using industry standard tools developed for HPGe detectors [6][7]. Industry has leveraged these advances, producing commercial, standalone CdZnTe systems with ~1% resolution [8]. Further improvements in CdZnTe readout and crystal selection has improved the energy resolution of commercial CdZnTe detectors to ~0.8% at 662 keV. Parallel improvements to CdZnTe detector packaging have greatly reduced system size and weight. The M400 detector combines both these advances, leveraging both improvements in energy resolution and system fieldability, as a new potential safeguards detector.

The capabilities of the M400 enable a new concept-of-operation for International Atomic Energy Agency (IAEA) safeguards inspectors. Most capabilities of two common IAEA inspector instruments, a robust, low-resolution NaI detector such as the identiFINDER2 HM-5 [9][10], and heavy, high-resolution HPGe detector, such as the Ortec µDetective [11], can be provided by a single M400 CdZnTe detector. Combining these instruments into a single, robust, medium-to-high-resolution detector would substantially reduce IAEA inspector burden and equipment costs. A proof-of-concept comparison between current IAEA safeguards equipment, competing medium resolution detectors, and the CdZnTe M400 for traditional safeguards measurements is made to explore this possibility.

CdZnTe M400 Detectors

M400 detectors consist of four CdZnTe crystals in a 2x2 array. Each CdZnTe crystal is instrumented with an 11x11 array of pixelated anodes and a planar cathode for 3-D position sensing. M400 modules are powered and readout via USB and ethernet. System weight and volume are 0.57 kg and 17.5 x 5.2 x 5.2 cm^3 respectively. A substantial fraction of system mass, 20%, and volume, 6%, are taken up by CdZnTe crystals which emphasizes the fieldability of M400 systems.

M400 detectors are held nominally at room-temperature through the use of an internal Peltier device. This Peltier draws the majority of system power in extreme, hot or cold, environments. Operation of similar

CdZnTe detectors has been demonstrated from -20-50°C. Additionally, M400 modules can be calibrated at other setpoints above or below room temperature, such as 35°C. These additional setpoints allow the system to run in a specific, non-room temperature environment without running the Peltier. Internal Peltiers may be completely removed in future design iterations by advanced calibration techniques.

Maximum M400 system throughput is around 30 kcps and limited by event readout and onboard processing. Currently, a single computer is used to readout all four crystals. An updated M400 detector, with independent readout of each of the four crystals, has been prototyped with a maximum count rate of around 120 kcps.

Measured Results

The performance of an HPGe detector (Ortec uDetective SN 18135981), 2x0.5" $LaBr_3$ scintillator readout by an MCA 527 (SN 1645) and CdZnTe M400 modules were directly compared by measuring check sources and special nuclear material standards in identical geometries at the IAEA. The two M400 modules, M0000005Dag and M0000006Thant, offered nominally similar performance. As such, the performance of only one CdZnTe system will be shown in each comparison for simplicity. Rough scale of each instrument is shown in Figure 1.

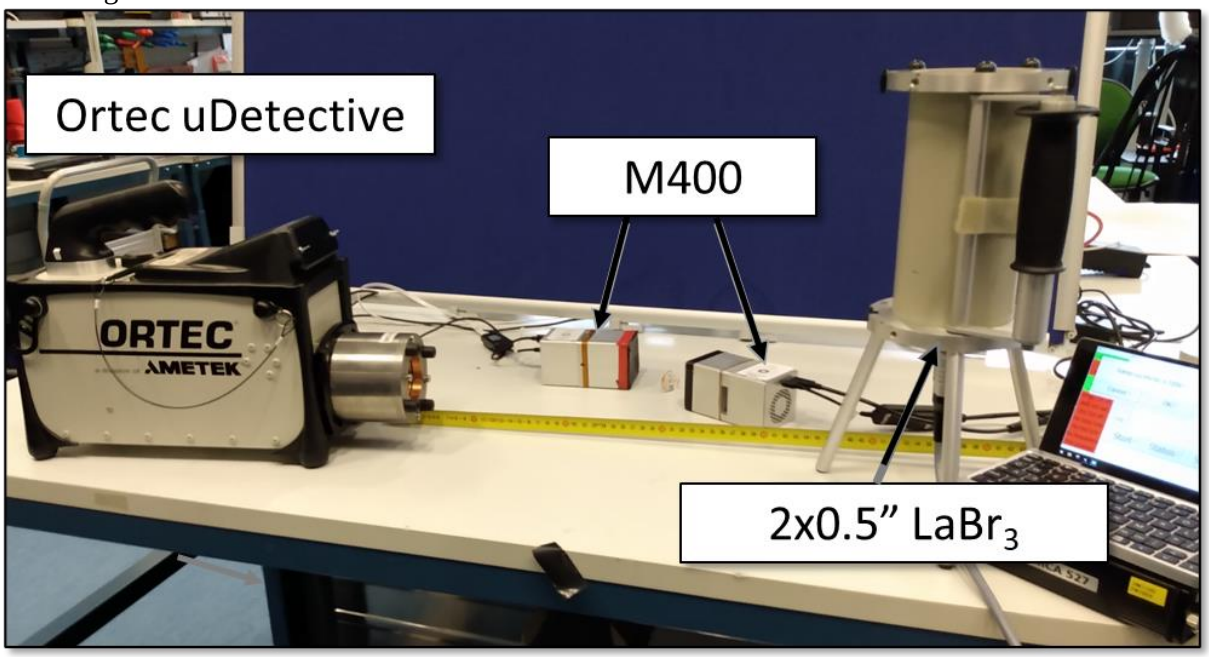

Figure 1: Ortec uDetective HPGe (left) two CdZnTe M400 modules (center) and a $LaBr_3$ scintillator readout using a MCA527 (right).

System throughput must be considered when fairly comparing the relative efficiency of each detector. Measured system throughput, for a variety of source types, is shown in Figure 2. The uDetective was found to be paralyzable, with relatively long per-event dead time. Note that the HPGe detector was configured to get the best possible energy resolution at the expense of system throughput. In contrast, both the M400 and $LaBr_3$ detectors were found to be non-paralyzable. Comparisons of high count rate sources, such as unshielded highly-enriched uranium (HEU), would unfairly penalize the HPGe detector using this low throughput setting.

As such, all subsequent comparisons were conducted at relatively low count rates where the effects of system efficiency and resolution, not dead time, were seen.

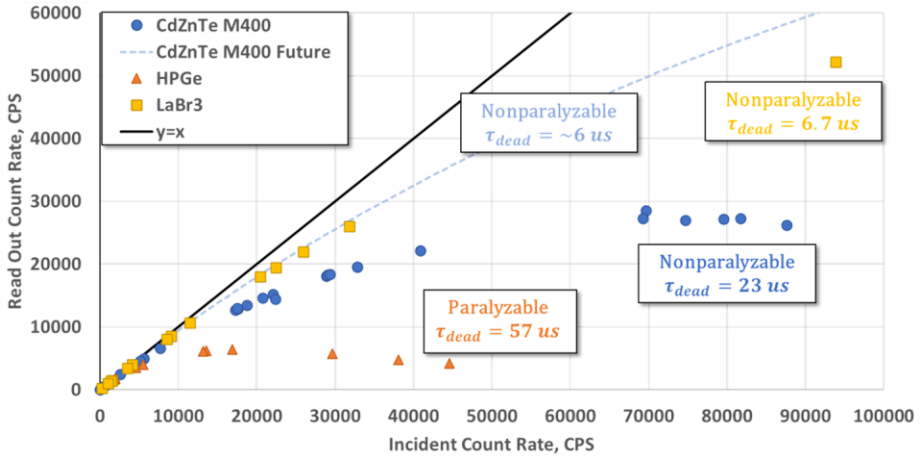

Figure 2: Measured system throughputs for samples of special nuclear material and lab check sources. The large dead time and paralyzable nature of the HPGe detector substantially limits event throughput on the uDetective: substantially higher HPGe throughput can be achieved with some resolution degradation. Note the upcoming M400 generation will have four-times lower dead time at a given incident count rate.

Detector performance was tabulated in *Table 1* at several key safeguards energies. 186 keV, an emission of ^{235}U, is used in both enrichment meter and non-constrained (FRAM-like) enrichment measurements. The 1001 keV emission of ^{234m}Pa, a decay product of ^{238}U, is similarly used in FRAM-like, efficiency curve-based analyses of uranium. The 642.4 keV emission of ^{240}Pu, around 662 keV, is used in the efficiency curve-based analysis of shielded plutonium. The CdZnTe M400 offers comparable surface area, which dictates efficiency at 186 keV in enrichment meter measurements, to the currently fielded HM-5 at ~8x better energy resolution. Similarly, the M400 offers substantially better energy resolution than even competing medium-resolution scintillators like $LaBr_3$. Comparisons against HPGe are less favorable, with energy resolutions varying from 2-3x times worse. However, CdZnTe spectra are still more-than-adequate for most FRAM-like analyses of uranium, and potentially plutonium, spectra.

Table 1: Comparison of the CdZnTe M400 and other currently fielded IAEA gamma-ray. HM-5 performance is estimated using GADRAS. SPD 500 performance is taken from literature. 186 keV efficiencies, from apples-to-apples measurements of depleted uranium, are meant for relative comparison only. An asterisk (*) represents currently fielded IAEA systems.

Detector	186 keV Efficiency, CPS	186 FWHM, keV	662 FWHM, keV	1001 FWHM, keV
uDetective* HPGe	236	1.2	1.3	1.6
M400 CdZnTe	145	2.4	4.0	5.0
2x0.5” $LaBr_3$	246	10.4	22.2	30.4
2x1.4” NaI (dentiFINDER2/HM-5)*	N/A	~20	~52	~65
SDP 500* CdZnTe	N/A	~3.2	~14	N/A

Uranium Measurements

Enrichment meter measurements are most complicated at low-enrichments. As such, detector spectra from a small depleted uranium (DU) standard behind 7 mm of steel are compared in Figure 3. This measurement is interesting as the weak 186 keV peak rides on a substantial, downscattered continuum. In realistic scenarios depleted uranium is stored in large casks, like the 48Y, such that downscatter of high-energy uranium gamma rays is even more intense around the 186 keV peak [12]. Steel shielding further attenuates the 186 keV line as shown in Figure 4. As such, energy resolution is critically important for accurately measuring the area of the 186 keV photopeak. The substantially worse resolution of $LaBr_3$ relative to CdZnTe (2.4 vs

10.4 keV FWHM at 186 keV) makes it difficult to accurately measure photopeak area in these scenarios. However, the $LaBr_3$ system was seen to have higher absolute efficiency. M400 CdZnTe systems can be easily tiled to match the absolute efficiency of even large 3" scintillators at 186 keV. In contrast, the uDetective was seen to have higher efficiency than the CdZnTe detector with better resolution. However, many enrichment meter measurements are currently conducted with NaI-based HM-5 detectors.

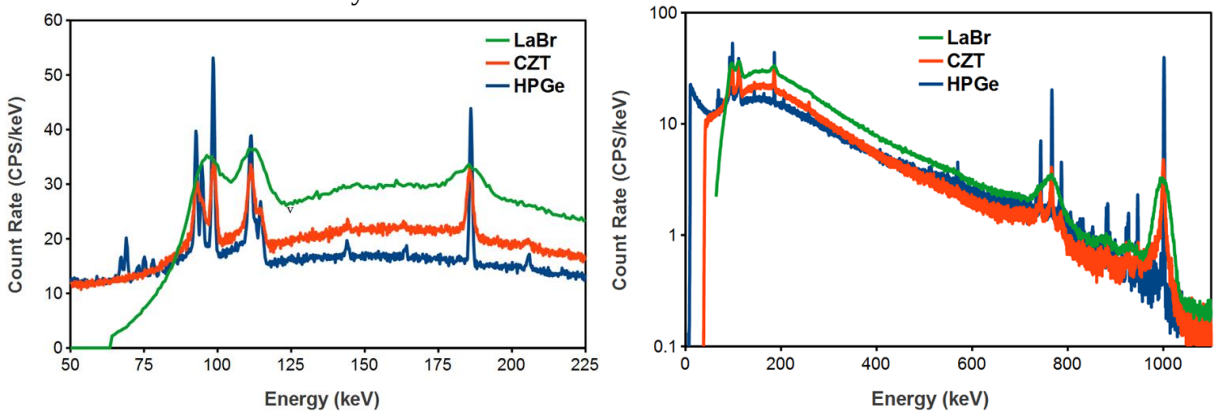

Figure 3: DU measured through a 7 mm steel shield using various detectors.

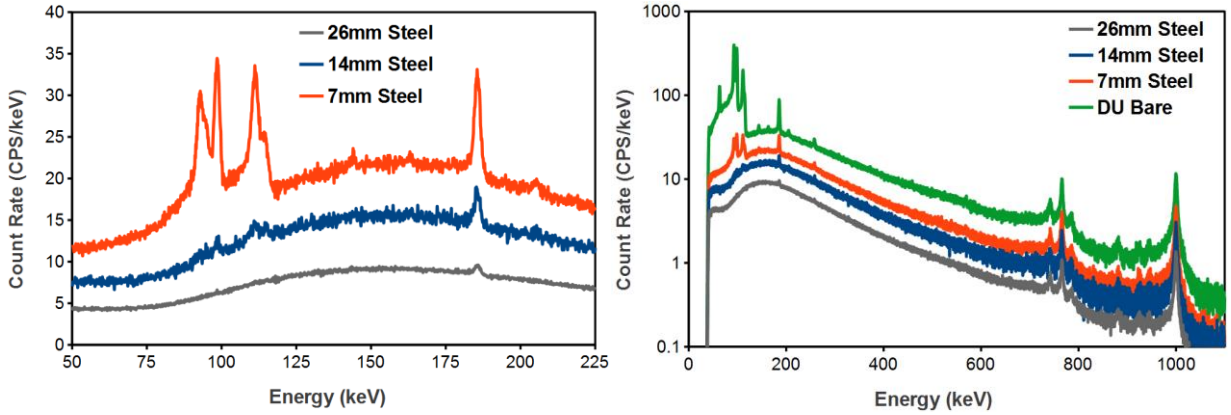

Figure 4: M400 CdZnTe DU spectra behind varying amounts of steel shielding. The 186 keV peak, which is more heavily attenuated, rides on top of a progressively larger, downscatter-heavy continuum with increasing shielding.

The performance of an M400-based enrichment meter was compared against a traditional 2x1.4" NaI detector, similar to that used in the HM-5, for shielded DU. Others have conducted similar analysis using RITEC CdZnTe detectors [13]. Detector spectra were simulated using GADRAS-DRF models of each detector and a predefined DU source (AIP1050Y2) behind 1 cm of iron [3]. Relative uncertainties in photopeak areas were computed using GADRAS's onboard peak fitting algorithm. Input peak fitting parameters were exactly those used to generate the data using the "inject" tool. Results from a 600 second integration at a source-to-detector distance of 25 cm at a 100 cm elevation off the ground are shown in Figure 5. Relative uncertainty in the NaI 186 keV photopeak area was found to be roughly 10x larger than that of the CdZnTe M400. This

suggests that M400 detectors would make superior enrichment meters, compared to standard NaI systems, in scenarios with shielded DU.

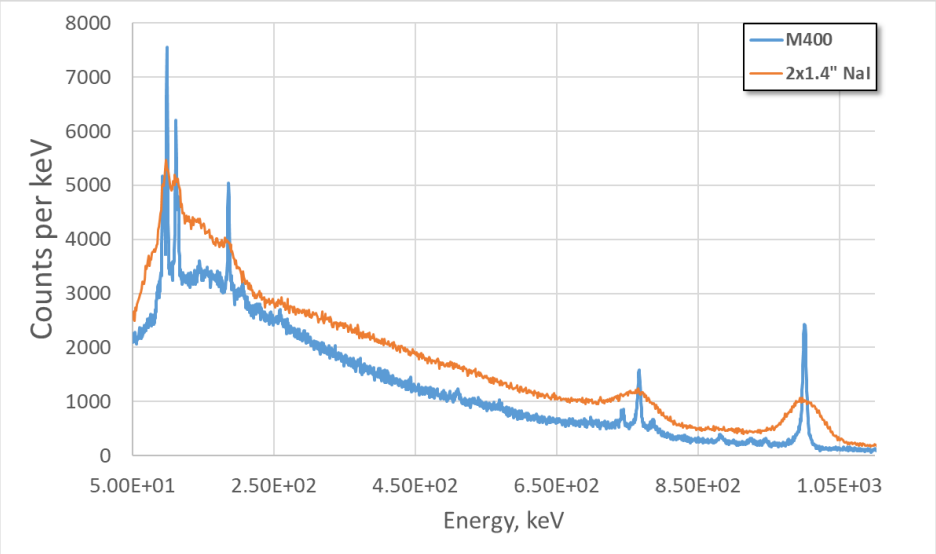

Figure 5: Apples-to-apples spectra from a CdZnTe M400 and 2x1.4" NaI detector for shielded DU. Spectra were simulated using the GADRAS-DRF AIP1050Y2 DU standard.

Estimates of uranium enrichment were also computed using the M400's onboard algorithm, which is run whenever the system detects uranium. Similar to FRAM, the technique uses energy-specific peak efficiencies, modulated by uranium and steel container thicknesses, to estimate uranium enrichment. The underlying algorithm is insensitive to gain shifts, which can be comparable to the 0.125 keV binning used in spectra, as photopeak centroids are calculated on a measurement-by-measurement basis from a robust isotope identification subroutine. When not all required peaks are detected, such as the 1001 keV peak in brief measurements of small quantities of HEU, a minimum detectable peak area is calculated and used in the enrichment estimate. Enrichment estimates for measured uranium standards with up to 26 mm of steel shielding are tabulated in Table 2 and plotted in Figure 6. Good agreement is seen between estimated and reported enrichments. A slight negative trend between iron thickness and estimated enrichment was seen. The cause of this trend is unknown but may stem from a mismatch in iron material definition.

*Table 2: Results from the M400 onboard uranium enrichment algorithm. Each standard was assumed to be thick relative to the mean-free-path of the 186/1001 keV emissions of uranium. Steel attenuation parameters were calculated using 304 stainless steel from the MCNP Material Compendium [14]. Uncertainties in peak areas used to compute enrichments were small. An * signifies enrichments calculated using estimated MDA values due to the lack of clear, high-energy peaks.*

True Enrichment, $\%^{235}U$	Steel Thickness, mm	Onboard Estimate, $\%^{235}U$
0.2	0	0.28
0.2	7	0.22
0.2	14	0.18
0.2	26	0.21
0.72	0	0.78
0.72	7	0.76
0.72	14	0.74
3.15	0	3.2
3.15	7	3.1
20.0	0	20.1
20.0	7	19.0

93.0	0	97.5*

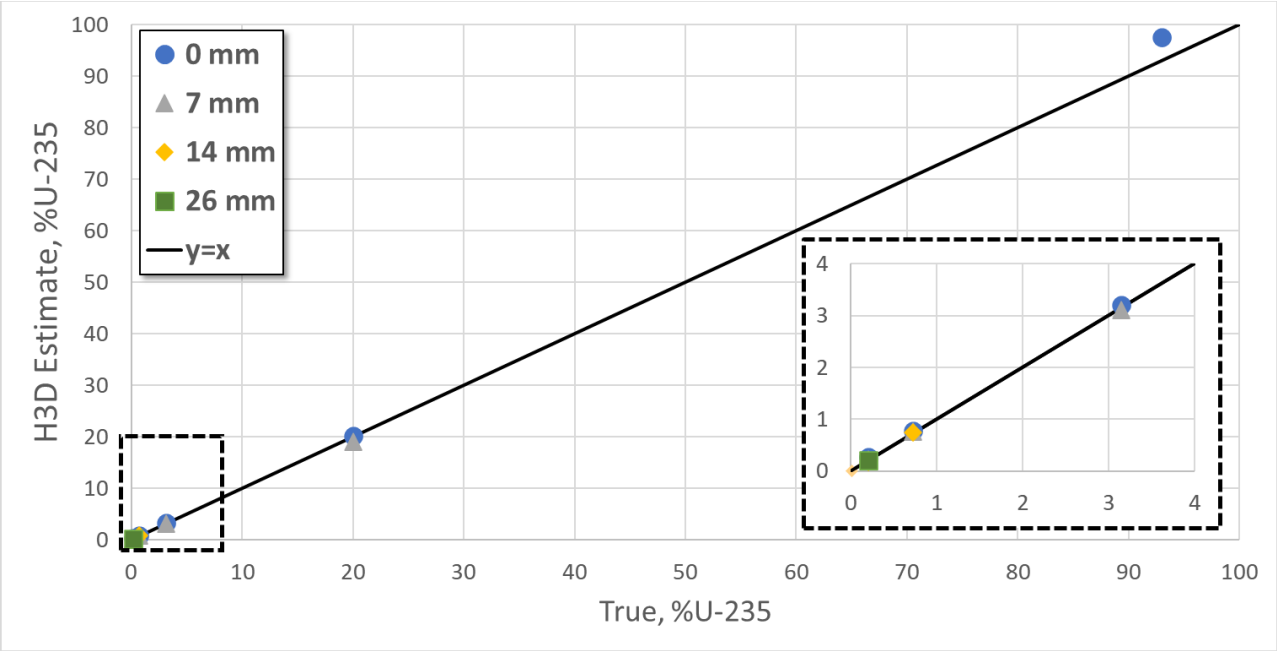

Figure 6: Estimates of uranium enrichment from Table 2. Perfect estimation is shown by the y=x line.

Plutonium Measurements

Similar analyses of reactor to weapons-grade plutonium (WGPu) are shown in Figure 7 and Figure 8. CdZnTe spectral features are once again found to be broader than HPGe but narrower than the $LaBr_3$ scintillator. Plutonium grading is far more difficult than measuring uranium enrichment. Plutonium measurements rely on FRAM-like analysis of cluttered spectra instead of enrichment meter approaches. Common HPGe-based plutonium analysis windows include 120-460 and 180-1010 keV. Extremely high energy resolution is required to adequately deconvolve ^{240}Pu peaks in the low-energy window: thus, low-energy analysis is typically performed with a planar HPGe detector. Previous CdZnTe systems have provided borderline grading performance using the higher-energy FRAMv5.2 window typically used by coaxial HPGe detectors [7]. However, CdZnTe peak shapes have now been added to FRAMv6.1 as shown in Figure 9. It is expected that this update will substantially improve the plutonium grading performance of CdZnTe detectors. Furthermore, the CdZnTe detector used in the FRAMv6.1 demonstration had substantially worse energy resolution (2.5 vs 0.8%) and lower volume (500 vs 19360 mm^3) than the M400 [15]. Spectra from identical plutonium standards are shown in Figure 10 to emphasize differences in system energy resolution. As such, pixelated CdZnTe plutonium grading performance should be reinvestigated now that FRAMv6, which includes CdZnTe peak shapes by default, has been released.

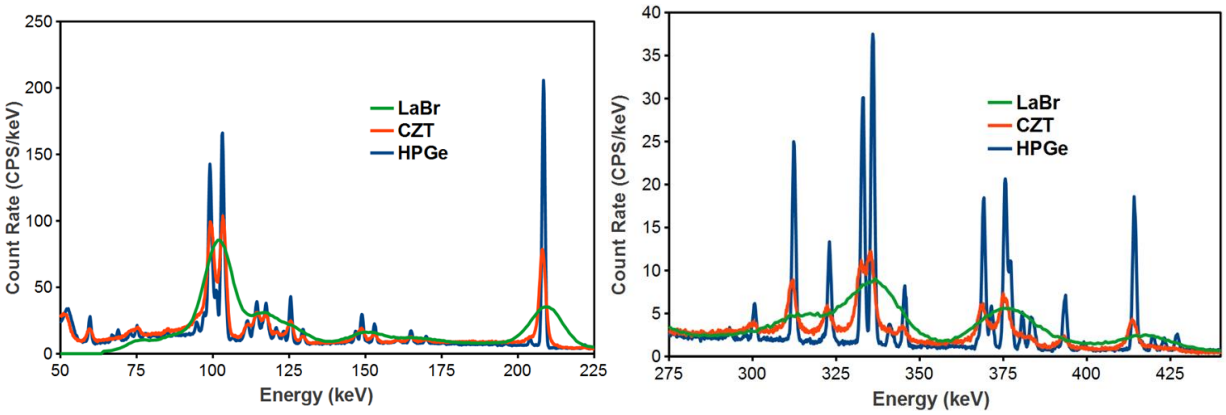

Figure 7: Pu61 CBNM standard (1.2% ^{238}Pu, 62.7% ^{239}Pu, 25.4% ^{240}Pu, 6.6% ^{241}Pu) measured on contact through a cadmium filter using each of the three detectors.

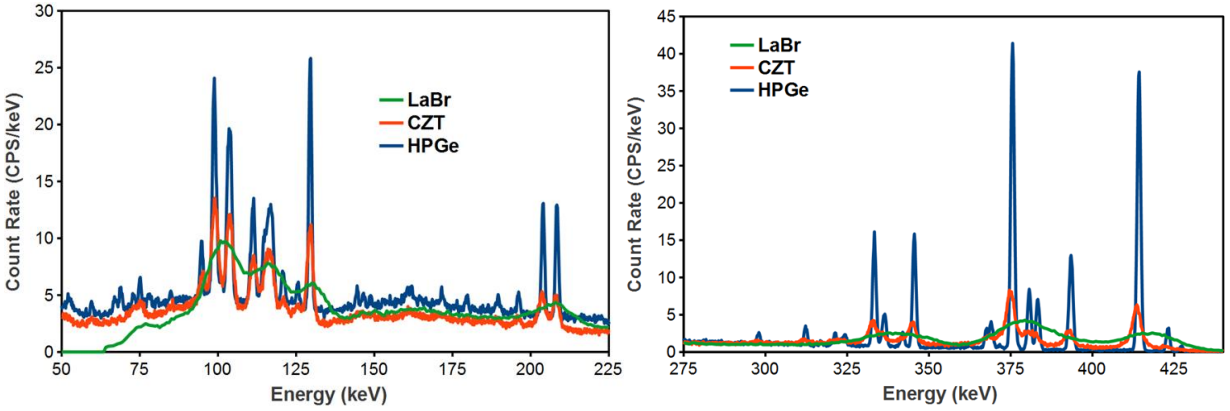

Figure 8: Pu93 CBNM standard (0.01% ^{238}Pu, 93.4% ^{239}Pu, 6.3% ^{240}Pu, 0.2% ^{241}Pu) measured on contact through a cadmium filter using each of the three detectors.

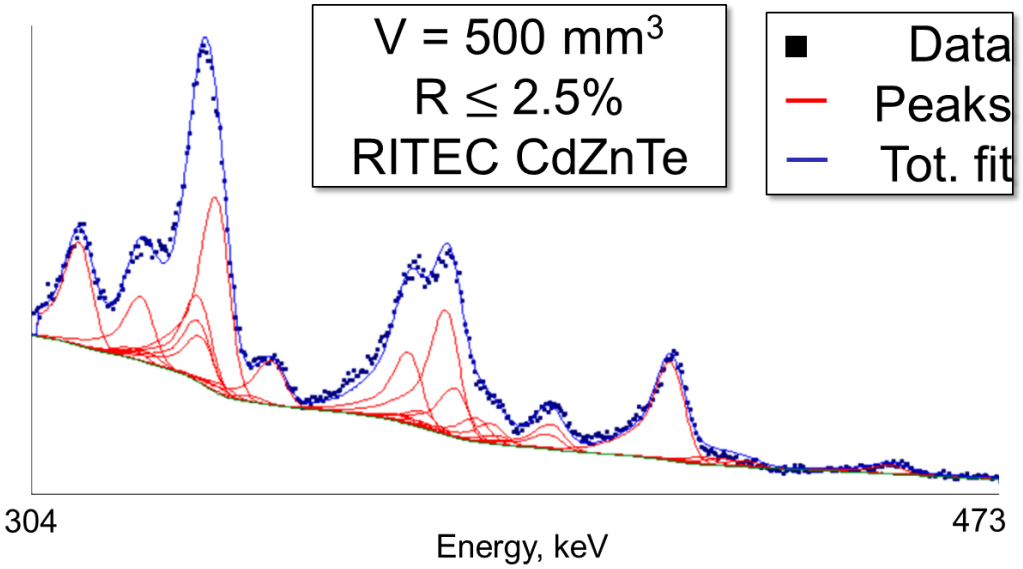

Figure 9: FRAMv6.1 fit of RITEC CdZnTe in the 304-473 keV window. Good agreement between measured spectra and the cumulative fit is seen. Base image taken from [16] and modified.

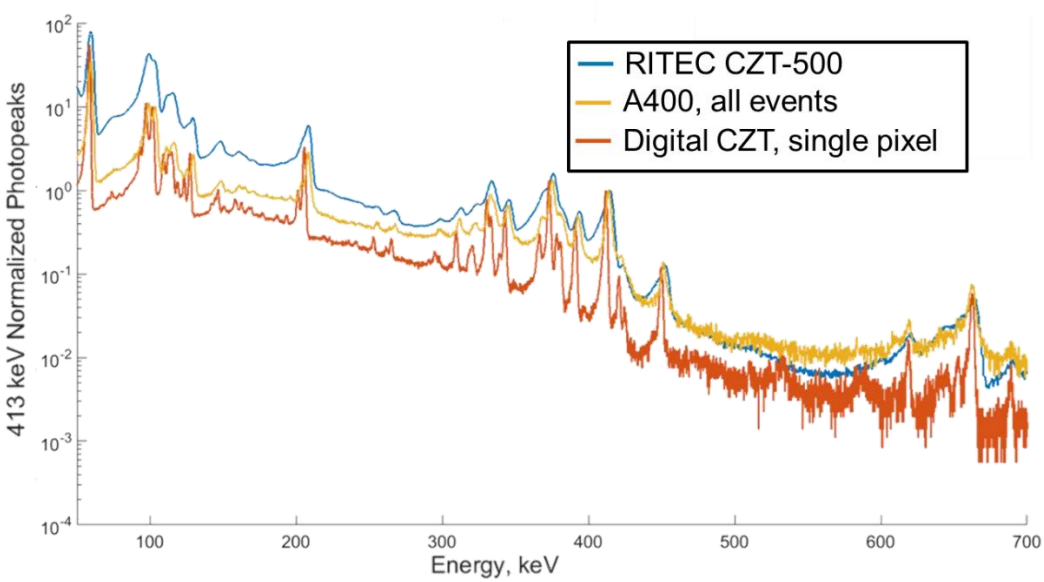

Figure 10: Comparison spectra from an A400, which is similar to the M400, and a RITEC CZT-500 on the plutonium standard CBNM Pu84. Slightly different tin or cadmium shielding was used between measurements to shield the 60 keV emission of ^{241}Am. A research, state-of-the art CdZnTe system from the University of Michigan using digital readout is also shown.

Conclusions

Modern CdZnTe detectors, like the M400, represent an attractive combination of desired traits from both rugged, low-resolution scintillators and fragile, high-resolution HPGe detectors. The M400 makes a compelling enrichment meter compared to currently fielded HM-5 detectors, providing ~10x lower uncertainty in 186 keV peak area in measurements of shielded DU. Previously, studies have shown the successful, unconstrained analysis of uranium enrichment using CdZnTe and FRAMv5.2, a task traditionally accomplished using HPGe. Onboard analysis of uranium grade showed good agreement across both uranium enrichment and shielding. Onboard plutonium grading is still under development while previous FRAMv5.2 studies using CdZnTe returned borderline results. However, CdZnTe-based analysis of plutonium should be vastly improved using FRAMv6.1 which includes intrinsic CdZnTe peak shapes. When improvements to FRAM for CdZnTe-based plutonium characterization are independently verified, M400 detectors can complete enrichment meter measurements better than current scintillators while simultaneously providing sufficient spectral quality for the unconstrained analysis of both plutonium and uranium traditionally done by HPGe. Combining the capabilities of both large, expensive instruments into a single, rugged detector offers the potential to greatly simplify the future concept-of-operations for IAEA inspectors.

Reference

[1] J. Sprinkle *et al.*, "Low-resolution Gamma-ray Measurements of Uranium Enrichment," Appl. Radiat. Isot., vol. 48, No. 10-12, pp. 1525-1528, 1997.
[2] Ortec, "FRAMv5.2: Plutonium and Uranium Isotopic Analysis Software," Accessed on Apr. 4, 2020. [Online]. Available: https://www.ortec-online.com/-/media/ametekortec/brochures/fram-a4.pdf
[3] R. Gunnink *et al.*, "MGAU, a new analysis code for measuring U-235 enrichments in arbitrary samples," IAEA symposium on International Safeguards, Vienna, Austria, March 8–14, 1994.
[4] S. M. Horne *et al.*, "GADRAS-DRF 18.5 User's Manual," tech. rep., Sandia National Laboratories, Albuquerque, New Mexico, 2014.
[5] M. Streicher, "Applications of Digitized 3-D Position-Sensitive CdZnTe Spectrometers for National Security and Nuclear Nonproliferation," Ph. D. Thesis, University of Michigan, 2017.

[6] D. Goodman, J. Xia, J. Sanders, Z. He, "FRAM v5.2 estimation of plutonium and uranium isotopics using digitized 3-D position-sensitive CdZnTe detectors," Nuclear Instruments and Methods in Physics Research A, 2018.
[7] D. Goodman, "Passive Characterization of Unknown Spaces Using Large-Volume Pixelated CdZnTe," Ph. D. Thesis, University of Michigan, 2019.
[8] C. G. Wahl *et al.*, "The Polaris-H imaging spectrometer," Nuclear Instruments and Methods in Physics Research A, vol. 784, pp. 377–381, 2015.
[9] V. Fournier, "What's in an inspector's luggage? A review of safeguards equipment," IAEA Bulletin, June 2016.
[10] IAEA, "Safeguards Techniques and Equipment: 2011 Edition," International Nuclear Verification Series No. 1 (Rev. 2).
[11] Ortec, "Micro-Detective: Ultra-Light, High-Fidelity Hand-Held Radioisotope Identifier." Accessed on Apr. 4, 2020. [Online]. Available: https://www.ortec-online.com/-/media/ametekortec/brochures/micro-detective.pdf
[12] R. Berndt, P. Mortreau, "^{235}U enrichment determination on UF_6 cylinders with CZT detectors," Nuclear Instruments and Methods in Physics Research A, vol. 886, pp. 40–47, 2018.
[13] V. Ivanov, J. Mintcheva, A. Berlizov, A. Lebrun, "Performance evaluation of new generation CdZnTe detectors for safeguards applications," IAEA (2015) IAEA-CN-220.
[14] R. McConn, C. Gesh, R. Pagh, R. Rucker, R. Williams, "Compendium of Material Composition Data for Radiation Transport Modelling," Technical Report; Pacific Northwest National Laboratory: Washington, DC, USA, 2011.
[15] RITEC, "CZT500," Accessed on Jun. 8, 2020. [Online]. Available: http://www.ritec.lv/html/czt500.html#specs
[16] D. Vo, T. Sampson, "Improvements of FRAM version 6.1," LA-UR-19-28449.